Journal of Power Sources 196 (2011) 6284–6292

Contents lists available at ScienceDirect

Journal of Power Sources

journal homepage: www.elsevier.com/locate/jpowsour

Three dimensional numerical simulation of gas–liquid two-phase flow patterns in a polymer–electrolyte membrane fuel cells gas flow channel

Y. Ding[a,b], H.T. Bi[a,b,*], D.P. Wilkinson[a,b]

[a] Department of Chemical and Biological Engineering, University of British Columbia, 2360 East Mall Vancouver, BC, V6 T 1Z3, Canada
[b] Clean Energy Research Centre, 2360 East Mall Vancouver, BC, V6 T 1Z3 Canada

ARTICLE INFO

Article history:
Received 22 February 2011
Received in revised form 30 March 2011
Accepted 31 March 2011
Available online 8 April 2011

Keywords:
PEMFC gas flow channel
Two-phase flow pattern
GDL microstructure
VOF method

ABSTRACT

Water management in polymer–electrolyte membrane fuel cells (PEMFCs) has a major impact on fuel cell performance and durability. To investigate the two-phase flow patterns in PEMFC gas flow channels, the volume of fluid (VOF) method was employed to simulate the air–water flow in a 3D cuboid channel with a 1.0 mm × 1.0 mm square cross section and a 100 mm in length. The microstructure of gas diffusion layers (GDLs) was simplified by a number of representative opening pores on the 2D GDL surface. Water was injected from those pores to simulate water generation by the electrochemical reaction at the cathode side. Operating conditions and material properties were selected according to realistic fuel cell operating conditions. The water injection rate was also amplified 10 times, 100 times and 1000 times to study the flow pattern formation and transition in the channel. Simulation results show that, as the flow develops, the flow pattern evolves from corner droplet flow to top wall film flow, then annular flow, and finally slug flow. The total pressure drop increases exponentially with the increase in water volume fraction, which suggests that water accumulation should be avoided to reduce parasitic energy loss. The effect of material wettability was also studied by changing the contact angle of the GDL surface and channel walls, separately. It is shown that using a more hydrophobic GDL surface is helpful to expel water from the GDL surface, but increases the pressure drop. Using a more hydrophilic channel wall reduces the pressure drop, but increases the water residence time and water coverage of the GDL surface.

1. Introduction

Water management is a critical aspect for improving the performance and durability of PEMFCs. The membrane needs to be sufficiently hydrated to maintain its high proton conductivity. Meanwhile, the excess water, existing as a liquid phase in the fuel cell, leads to so-called "flooding" in the catalyst layers, gas diffusion layers (GDLs) and gas flow channels, which may block the reactant pathway and reduce the fuel cell performance. The presence of liquid water in the PEMFC gas flow channel results in gas–liquid two-phase flow and can cause parasitic energy loss, flow maldistribution and poor performance. Therefore, it is important to study the two-phase flow phenomena that occurs in the gas flow channels in order to mitigate its negative effects.

The gas–liquid two-phase flow in PEM fuel cell channels is quite unique compared to other conventional two-phase flows. For example, water enters the channel from random pores of porous GDLs, rather than from the front of fixed positions; the channel wall materials have different properties; and the gas–liquid flow ratio is about 10^4, which is much larger than those in regular two-phase flow applications, e.g. pipe flows, chemical reactors and heat exchangers. As revealed in a recent review by Anderson, et al. [1] on gas–liquid two-phase flow phenomena in gas flow minichannels and microchannels related to PEM fuel cell applications, although extensive work has been done on this subject, both experimentally and computationally, there is still more work required, e.g., to identify and predict the two-phase flow patterns and regimes in an operating PEM fuel cell.

The two-phase flow pattern in PEMFC gas flow channels has a great impact on the reactant distribution and the pressure drop. Several flow patterns have been found in the PEM fuel cell channel both from in situ [2,3] and from ex-situ [4,5] experiments, such as mist flow, droplet flow, film flow, annular flow and slug flow. Hussaini and Wang [3] and Lu et al. [5] also developed two-phase flow regime maps in terms of superficial gas and liquid velocities. These flow regime maps are useful for selecting optimal operating conditions. However, the two-phase flow pattern depends not only on the gas and water flow rate, but also the channel design and operating procedure, etc. For example, the two-phase flow maldistibution in multiple channels [6] and flow hysteresis have been

* Corresponding author at: Department of Chemical and Biological Engineering, University of British Columbia, 2360 East Mall Vancouver, BC, V6 T 1Z3, Canada. Tel.: +1 6048224408; fax: +1 604 822 6003.
E-mail address: xbi@chbe.ubc.ca (H.T. Bi).

0378-7753/$ – see front matter © 2011 Elsevier B.V. All rights reserved.
doi:10.1016/j.jpowsour.2011.03.100

found to be closely related to the flow patterns [7–9]. The two-phase flow pattern may also vary along the length of the channel, since water is constantly introduced into the channels from the GDL. Different GDL materials also change the two-phase flow patterns in the channel [10]. Meanwhile, current experimental work cannot exactly reproduce the two-phase flow in an operating PEM fuel cell due to the limitations of visualization techniques. So far, the most common technique is to use a transparent fuel cell. However, the transparent materials used in the cell usually are very different from those employed in the fuel cell, with different properties with such as the material contact angle and roughness. Other techniques, such as magnetic resonance imaging, neutron imaging and X-ray techniques, do not involve transparent materials, but have very low spatial and temporal resolution compared to the optical photography method [11]. Therefore, the existing studies of two-phase flow patterns in PEM fuel cell channels still lacks consistency in the literature.

On the other hand, it is quite difficult to obtain quantitative information from experimental work, such as the liquid water volume fraction and GDL water coverage ratio, which are key parameters having negative effects on the PEM fuel cell performance. Computational modeling and simulation, is a powerful alternative method that is often able to provide more details and quantitative results. It is convenient to observe the formation and transition of two-phase flow patterns inside the channel. The pivotal issue in modeling and simulation is the two-phase flow model. Since 2000, several two-phase models have been incorporated in the fuel cell modeling [12,13], such as the mixture model [14,15], the multi-fluid model [16,17], and the volume of fluid (VOF) method [18]. Among different two-phase models, the VOF method is the most powerful tool to simulate the two-phase flow patterns in the PEM fuel cell channels, since it is able to consider the surface tension and wall adhesion effects and to track the shape of a droplet, which is the main form of the water emerging from the GDLs [19]. So far, the VOF method has been widely used to simulate various two-phase flow phenomena in the PEM fuel cell, such as single droplet formation and motion [19–21], parametric studies on the effects of material wettability, gas or liquid velocity, contact angle hysteresis and surface tension [20,22–27], novel gas flow channel designs [28–31], even coupled with electrochemical reactions, and heat transfer and species transport to model a PEM fuel cell unit [32,33]. To the author's knowledge, the formation and transition of the two-phase flow patterns in PEM fuel cell channels has not been simulated in the open literature. The main difficulty of such a simulation is how to consider the GDL microstructure. Most of the simulations do not address this issue, and have treated the GDL surface either as a homogenous surface or a surface with only a single open pore for liquid water injection. Some pore-scale models, such as the pore-network model and the Lattice Boltzmann model, are able to consider the detailed microstructure of the GDL, but at the micro-scale, which is thus not suitable for simulating the two-phase flow patterns at the macro-scale that form in the flow channel.

In our previous work [34], a simplified microstructure for the GDL surface was proposed in order to simulate the multiple droplet behavior in a microchannel of a PEMFC. It was found that, in the channel width direction, at least 2 pores are required to represent the microstructure of the GDL surface, and the two-phase flow pattern in the channel does not change with any further increase in the pore number or decrease in the pore diameter at a constant GDL surface porosity. In this work, we extended the previous work by implementing the simplified microstructure to a much larger channel, which is comparable with realistic PEMFC gas flow channels. The effects of liquid injection rates and surface wettability on two-phase flow patterns in the flow channel were investigated based on simulation results.

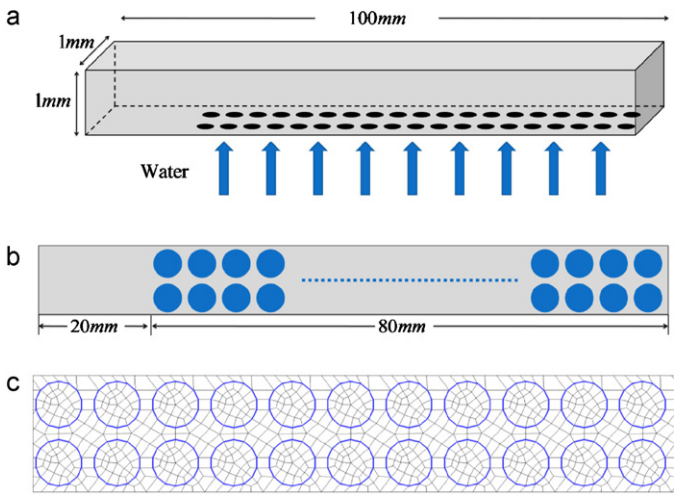

Fig. 1. Three-dimensional computational domain: (a) overview (b) simplified GDL microstructure (c) Local view of GDL microstructure with meshes.

2. Numerical method

The three-dimensional computational domain is shown in Fig. 1(a) cuboid channel, which is used in all the simulations, has a 1.0 mm × 1.0 mm square cross section and is 100 mm in length with a hydrophobic GDL surface on the bottom and three hydrophilic channel walls. There is a 20 mm long entrance region before the water emergence area, which ensures the gas flow being fully developed before contacting the water droplets. In our previous simulation work [34], it was shown that two pores in the width direction are enough to represent the microstructure of the GDL surface in a microchannel. Therefore, in this work, the same strategy is employed to simplify the GDL surface structure by opening 320 pores on the GDL surface with the same diameter of 400 μm. The criterion for the selection of 400 μm pore diameter is to ensure that the total open area of GDL surface is around 50%, the porosity of typical GDL surfaces [35]. Air flows into the channel from one end and liquid water is injected from the multiple pores along the GDL surface.

For the base case, the velocity of air was set at 5 m s^{-1} at atmospheric pressure, which is of the same order of magnitude as flows encountered in automotive fuel cell stacks [25]. The liquid injection velocity was set at 10^{-4} m s^{-1} for all the pores, which corresponds to the theoretical liquid generation rate at a current density of 0.5 A cm^{-2}. Laminar flow and the non-slip boundary condition are assumed since the Reynolds number of each phase is quite small (Re_g = 458, Re_l = 11.9). The static contact angles of GDL surface and channel wall surface were set at 140° and 45°, respectively, based on typical PTFE treated carbon paper GDL materials and carbon plate [35]. Air and water physical properties, i.e., densities, viscosities and surface tension coefficient were all set to a typical PEM fuel cell operating temperature of 70 °C. The model is isothermal, with liquid evaporation and condensation being unaccounted. The time step for the baseline simulation was set at 10^{-6} s, which ensures that the global courant number is less than 1. 149,690 meshes in total were used in the simulation with a mesh size of 0.1 mm. Fig. 1(c) shows the local view of meshes at water inlet and GDL surface. Time step and mesh size independency were examined for the base case, to prove that they were small enough. The VOF method was implemented using the commercial software, FLUENT® 6.3.26. The geometric reconstruction scheme was used to represent the interface between two fluids. All the related model equations can be found in our previous work [34] and the software user's manual [36]. The build-in VOF method in FLUENT was already validated

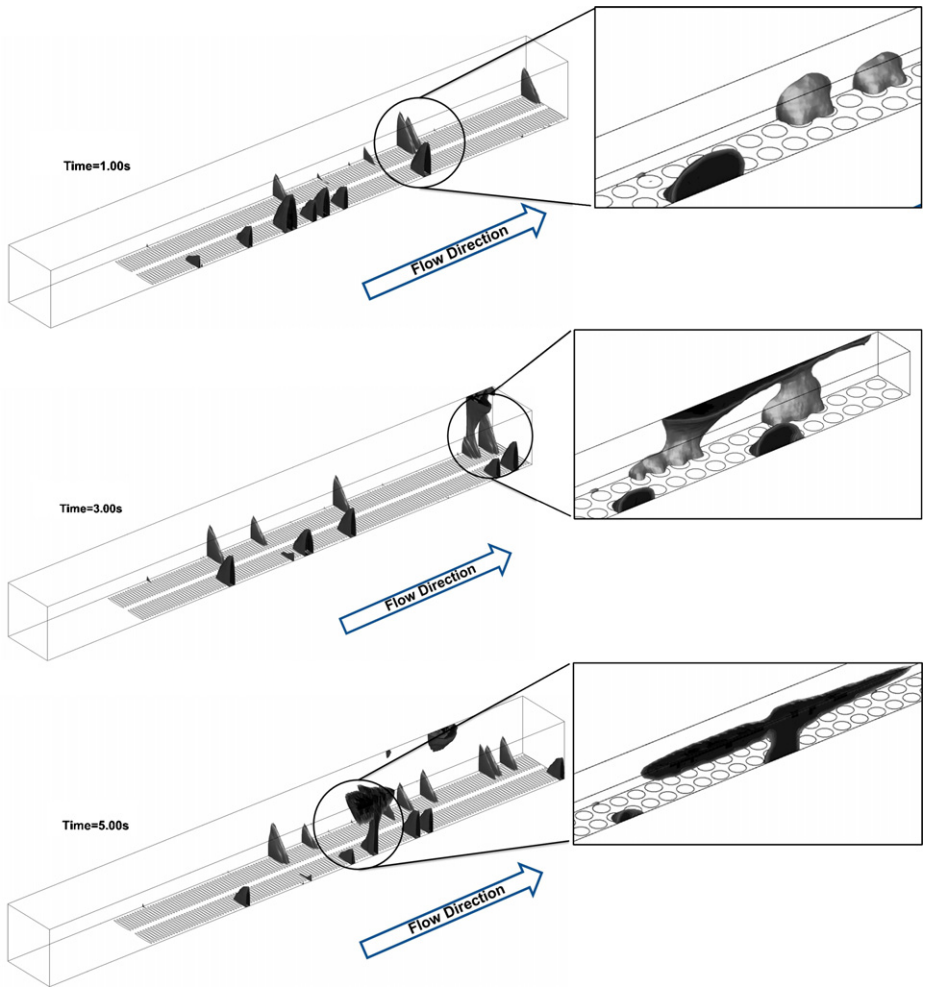

Fig. 2. Two-phase flow patterns in the channel.

against experimental results by Le et al. [37] based on the comparison of simulated and measured two-phase flow patterns and overall pressure drops in the serpentine channel of a PEM fuel cell.

3. Results and discussion

3.1. Two-phase flow patterns in gas flow channel

It is worth noting that since the length to height ratio of the channel is 100:1, it is difficult to have an overview of the whole channel. Therefore, for a better view, the length of the channel has been suppressed by a factor of 10 times, making the spherical droplets ellipsoid-like. Meanwhile, the undistorted two-phase flow patterns at certain location are also given by snapshots besides the overall view.

As shown in Fig. 2, for the base case, the three-stage droplet behavior, which was found in our previous work, namely emergence and merging of liquid water on the GDL surface, accumulation on the side walls, and detachment from the top wall, could be indentified in the channel. Liquid droplets first emerge from the pores and then coalesce on the GDL surface to form larger droplets. Due to the wettability difference between the GDL surface and channel walls, droplets on the GDL surface tend to attach to side walls (emergence and merging stage). Then, as the liquid water is constantly injected from the bottom, more and more water accumulates on the side wall, resulting in even larger droplets (accumulating stage). Due to the drag force exerted by the gas, large droplets begin to move slowly along the side wall, which forms so-called bottom corner droplet flow on the GDL surface. As these droplets move forward, more and more droplets coalesce and the droplets grow larger. Once a droplet hits the top wall, it rapidly

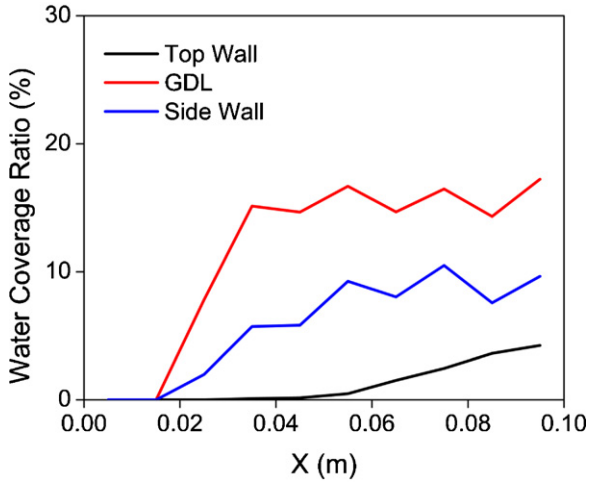

Fig. 3. Time-averaged water coverage ratio on different surfaces along the channel.

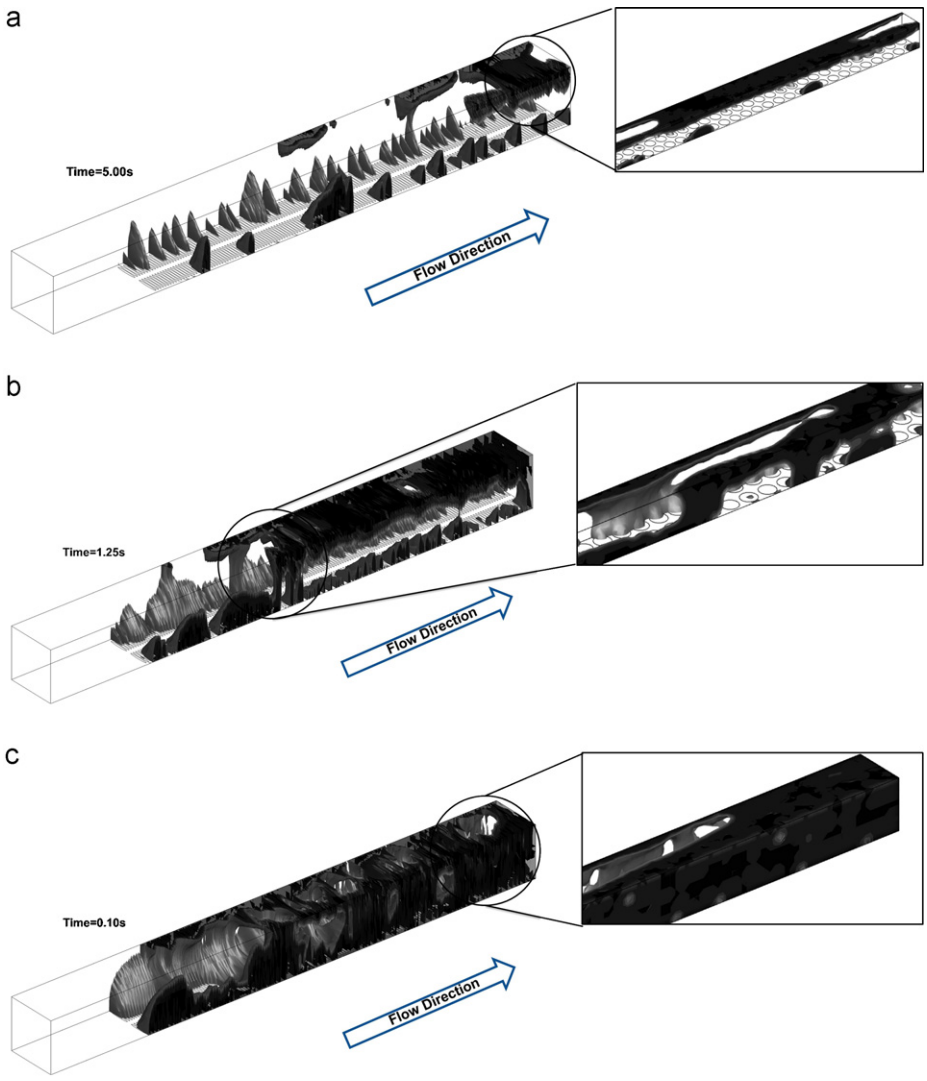

Fig. 4. Effects of liquid flow rate on the two-phase flow patterns in the channel: (a) ×10 case, (b) ×100 case, and (c) ×1000 case.

spreads out on the top wall, and due to its much faster speed, it quickly detaches itself from the bottom corner, with some water on the side wall also being dragged away (detachment stage). As a result, corner droplet flow is formed. Since the droplet on the top wall moves much faster, it gives them more opportunities to coalesce with other droplets that are still sitting on the bottom corner. Therefore, droplets flow on the top corner are usually larger than those on the bottom corner.

To quantitatively illustrate the two-phase flow pattern evolution along the channel, the time-averaged water coverage ratio on different surfaces along the channel was calculated as shown in Fig. 3. The *x*-axis indicates the distance from the channel inlet, and the water coverage ratio is defined as the ratio of the surface area covered by water to the total surface area. The GDL water coverage ratio is more important since the water on the GDL surface blocks the reactant diffusive pathway. To maintain a good cell performance, GDL water coverage should be kept as low as possible. In this case, the high GDL water coverage ratio means that the flow pattern is mainly bottom corner flow. The fluctuation in water coverage on the GDL and side wall reflects the droplet detachment from the bottom. The top wall water coverage ratio is still increasing, indicating that the flow is still developing along the channel.

3.2. Effects of liquid flow rates

In the base case, the liquid injection rate was set according to the theoretical liquid generation rate by the electrochemical reaction in the cathode catalyst layer using dry air as the reactant gas. Practically, the inlet gas is usually humidified to avoid membrane dehydration. Therefore, the liquid water formation rate in the cathode side channel is usually much higher than that generated by the reaction due to water condensation. Also, in an active PEM fuel cell the gas channel is much longer, and more water tends to accumulate in the channel especially in the downstream section of the channel, resulting in various two-phase flow patterns as observed in the literature. However, simulating such a long channel requires an extremely huge computational time. To shorten the water accumulation, we simply increased the liquid injection rates by 10 (×10 case), 100 (×100 case) and 1000 (×1000 case) times, respectively to mimic the flow patterns in the downstream section of a long channel.

The two-phase flow pattern for each case is shown in Fig. 4, and the time-averaged water coverage ratio on different surfaces along the channel is shown in Fig. 5. For the ×10 case (Fig. 4a), droplets emerge into the channel much faster than that in the base case (Fig. 2), resulting in more and bigger droplets on the GDL surface.

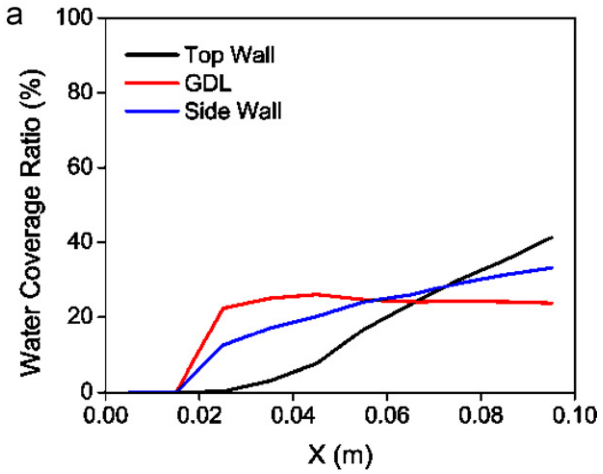

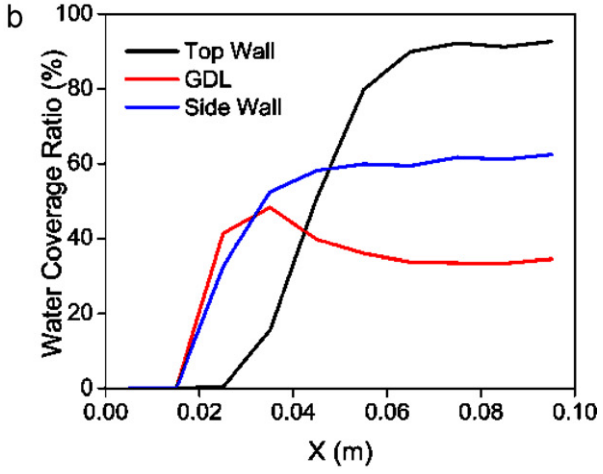

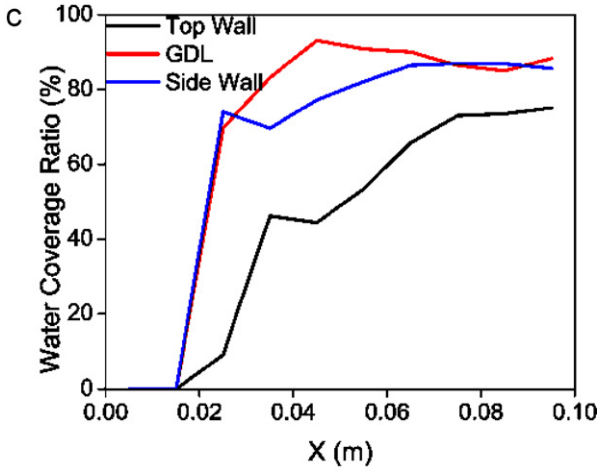

Fig. 5. Time-averaged water coverage ratio on different surfaces along the channel: (a) ×10 case, (b) ×100 case, and (c) ×1000 case.

Meanwhile, the detachment occurs more frequently, with more water flowing on the top wall. Since the top wall is hydrophilic, the droplets in the top corner tend to form a liquid film. Therefore, the flow pattern for the ×10 case is bottom corner droplet flow and top wall film flow. Fig. 5a shows that the GDL surface water coverage ratio reaches its highest point at about 0.04 m, indicating that beyond this point, droplets detach faster than they emerge. The top wall water coverage ratio begins to exceed the GDL surface water coverage ratio at about 0.065 m, and it still continues to increase at the end of channel, indicating that the flow is still developing. Further increasing the liquid flow, as shown in the ×100 case (Fig. 4b), results in more water present on all the channel walls. Droplets on the GDL surface merge together and the liquid film on the top wall covers almost all the top wall surface, which makes the flow pattern in the channel similar to annular flow. The water coverage ratio on each wall eventually becomes stable as shown in Fig. 5b. Most of the water flows on the top wall, which results in the GDL water coverage ratio being similar to the ×10 case. When the liquid flow rate is amplified by 1000 times, quite distinct flow patterns are formed in the channel (Fig. 4c). Liquid water covers almost all the channel wall surface, and becomes a continuous phase. An annular flow pattern develops in the entrance section, and then gas bubble and slug flow are identified in the exit section of the channel. Due to the density differences between water and air, discrete gas bubbles can easily escape from the top of the channel. Therefore, the GDL surface water coverage ratio is much higher than that of the top wall (Fig. 5c), which indicates a much different water distribution for very high water injection rate.

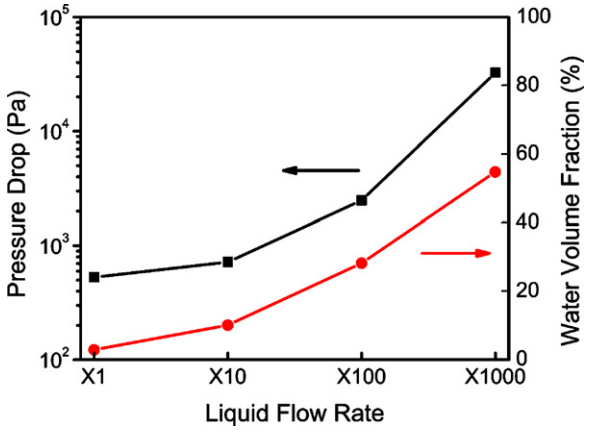

Fig. 6. Effects liquid flow rate on the pressure drop and water volume fraction in the channel.

These selected four cases imply that, the flow patterns in a longer PEM fuel cell flow channel may follow a flow pattern evolution along the length of channel, namely, corner droplet flow at the beginning of channel, followed by top wall film flow, annular flow, and finally slug flow in the channel. From a practical point of view, slug flow should be avoided as much as possible, since it causes an extremely high GDL surface water coverage ratio and therefore significant loss in fuel cell performance.

The effects of liquid flow rates on the time-averaged water volume fraction (also called water saturation) and total pressure drop were also analyzed as shown in Fig. 6. The water volume fraction or the water saturation indicates the degree of channel flooding. The pressure drop, which is a key parameter, indicates the energy loss for the fluid flowing through the channel. It is obvious that the pressure drop increases exponentially with the increasing water volume fraction, water accumulation in the channel for an operating PEM fuel cell should be avoided as much as possible to reduce parasitic energy loss, reactant flow maldistribution, and poor cell performance.

3.3. *Effects of GDL surface wettability*

The wettability of the GDL, which is characterized by the surface contact angle, plays a significant role in PEM fuel cell water management. To investigate the impact of GDL surface wettability on the two-phase flow patterns formed in the channel, several GDL

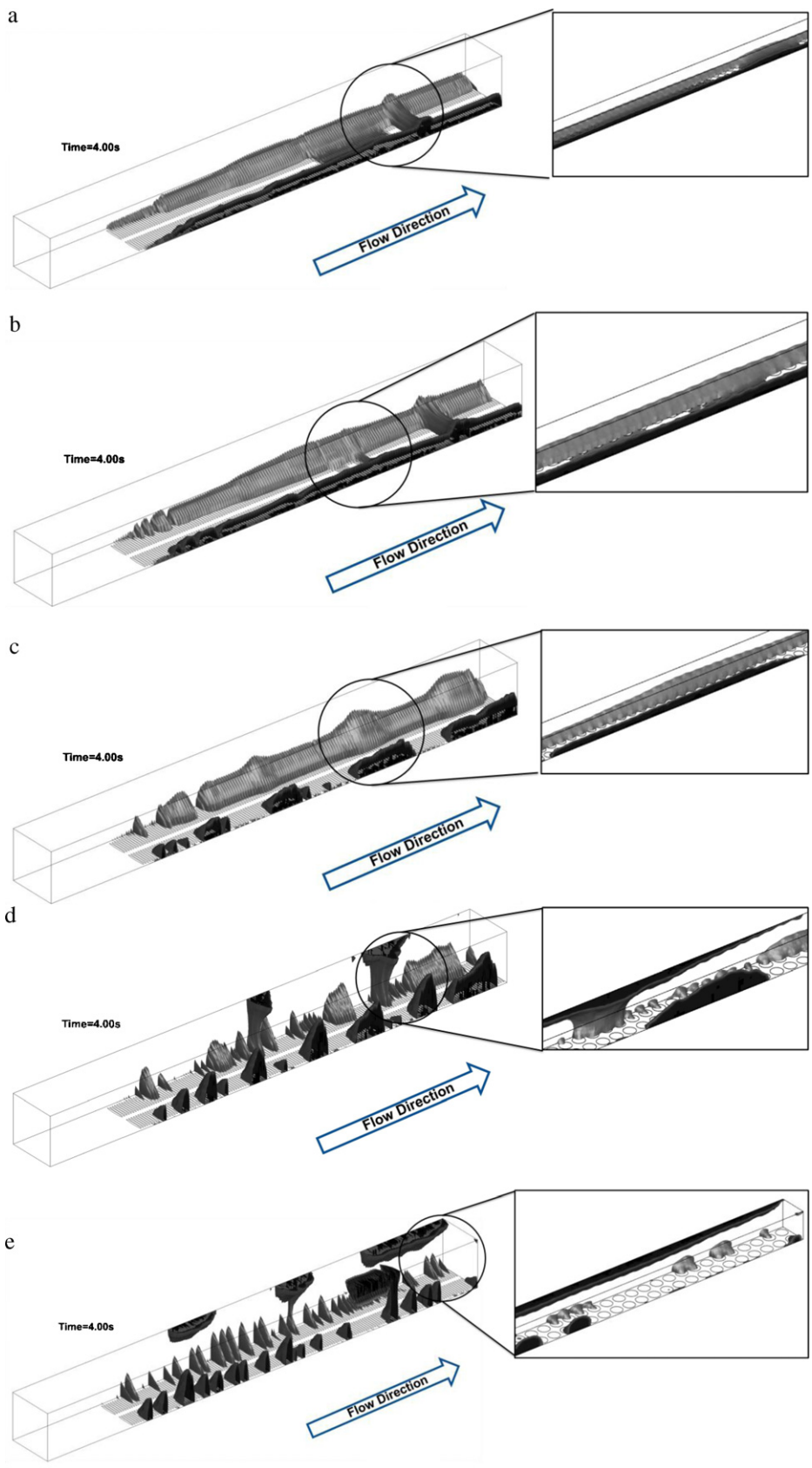

Fig. 7. Effects of contact angle of GDL surface on the two-phase flow patterns in the channel: (a) $\theta = 45^\circ$, (b) $\theta = 60^\circ$, (c) $\theta = 90^\circ$, (d) $\theta = 120^\circ$, (e) $\theta = 140^\circ$.

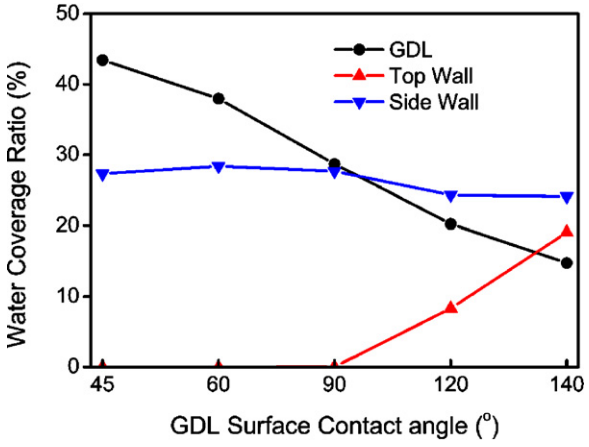

Fig. 8. Effects of GDL surface contact angle on the water distribution in the channel.

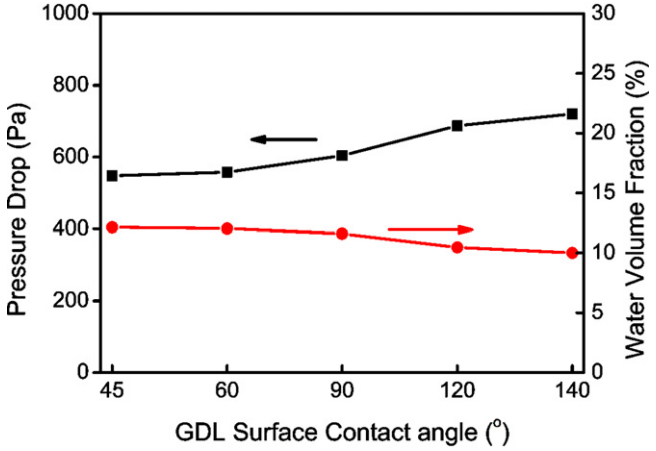

Fig. 9. Effects of GDL surface contact angle on the pressure drop and water volume fraction in the channel.

surface contact angles, i.e., 45°, 60°, 90°, 120°, and 140° were tested in the simulation. The contact angle of the other walls was kept constant at 45°. The liquid water injection rate was amplified by 10 times as in the ×10 case. Fig. 7 shows quite different two-phase flow patterns in the channel for different GDL contact angles. When the GDL surface contact angle is hydrophilic, i.e., Fig. 7a, b, c, water on the GDL surface tends to form a liquid film. The lower the GDL contact angle, the higher the GDL area that is covered by the water, which blocks the reactants pathway to the catalyst layer and leads to decreased fuel cell performance. There is no water flowing on the top wall for these hydrophilic cases. Therefore, the flow pattern in the channel is bottom film flow or bottom corner flow. As the contact angle of the GDL surface increases, liquid water begins to move to and accumulate on the side walls, and the higher the contact angle, the more water moving from the GDL surface to the side walls. When the GDL surface is hydrophobic, i.e. Fig. 7 d, e, water begins to form liquid droplets rather than liquid films, and the three-stage droplet behavior can be identified again. The two-phase flow pattern becomes corner droplet flow as observed in the base case.

The effects of GDL wettability on the time-averaged water distribution are shown in Fig. 8. For the hydrophilic GDL surface, the water coverage ratio on the side walls changes very little with varying GDL contact angle due to the balance of liquid droplet moving from the GDL to the side wall and faster expelling out of the channel. No water is present on the top wall, and the water coverage ratio on the GDL surface decreases significantly as the contact angle increases. This is because a higher contact angle lifts the water up, changing the water on the GDL from a liquid film to droplets, thus occupying less GDL surface area. On the other hand, for the hydrophobic GDL surface, further increase in contact angle decreases the water coverage ratio on the GDL surface. Meanwhile, the liquid droplets are able to touch the top wall, resulting in the top corner flow, which decreases the water coverage ratio on the side walls slightly.

The effects of GDL surface wettability on the time-averaged pressure drop and water volume faction are shown in Fig. 9. Increasing the GDL surface contact angle always increases the total pressure drop, which is consistent with experimental results in the literature [38,39]. This is because higher hydrophobicity of the GDL surface lifts more water up from the GDL surface to occupy more of the cross sectional channel area, which blocks the gas pathway in the channel, resulting in higher pressure drop. In addition, the increased drag forces between the liquid and gas also shorten the water residence time in the channel and thus reduce the water volume fraction.

It can be concluded from the previous observations that increasing the hydrophobicity of the GDL surface is helpful to expel liquid water from the GDL surface and reduce the water volume fraction in the channel, but the pressure drop also increases slightly. Therefore, in the selection of the GDL contact angles both avoiding flooding and reducing parasitic energy loss should be considered.

3.4. Effects of channel wall surface wettability

The effects of channel wall surface wettability were also investigated by varying the contact angle of channel walls from 45° to 140°, i.e., 45°, 60°, 90°, 120°, and 140°. The contact angle of the GDL surface was kept at 140° for all these cases. The liquid water injection rate was amplified by 10 times as in the ×10 case. Fig. 10 shows the two-phase flow patterns formed in the channel for different channel wall contact angles. For hydrophilic channel walls (Fig. 10 a–c), the flow pattern is corner droplet flow as observed in the base case. For more hydrophilic wall surfaces, the droplets on the GDL surface move more easily to the top wall, increasing the droplet detachment frequency and forming larger droplets on the top corner, thus, facilitating faster water removal from the channel. For hydrophobic channel walls (Fig. 10 d, e), the flow pattern is droplet flow on the GDL surface, and no water flows on the top wall. All the droplets are expelled from the hydrophobic surfaces, occupying a large cross sectional area of the channel, and thus become easier to be flushed out by the gas. It is also observed that the highly hydrophobic channel walls can further prevent the formation of larger droplets in the channel and reduce the droplet resident time.

The effects of channel wall wettability on the water distribution in the channel are shown in Fig. 11. It is found that when the channel wall is hydrophilic, increasing the channel wall contact angle significantly decreases the water coverage ratio on the top and side walls, due to the prevention of droplet formation on the side walls. Correspondingly, the GDL surface coverage also decreases slightly, since the larger droplets formed on the GDL surface accelerate their removal from the channel. When the channel wall is hydrophobic, stable droplets are formed, with little water attached onto the top and side walls. Therefore, any further increase in the channel wall contact angle has little impact on the water distribution in the channel.

The effects of channel wall wettability on the pressure drop and water volume fraction are shown in Fig. 12. The pressure drop is seen to increase first with increasing the channel wall contact angle due to the larger water cross sectional area, followed by a slight decrease due to the smaller droplets formed on the GDL surface. Increasing the channel wall contact angle always decreases

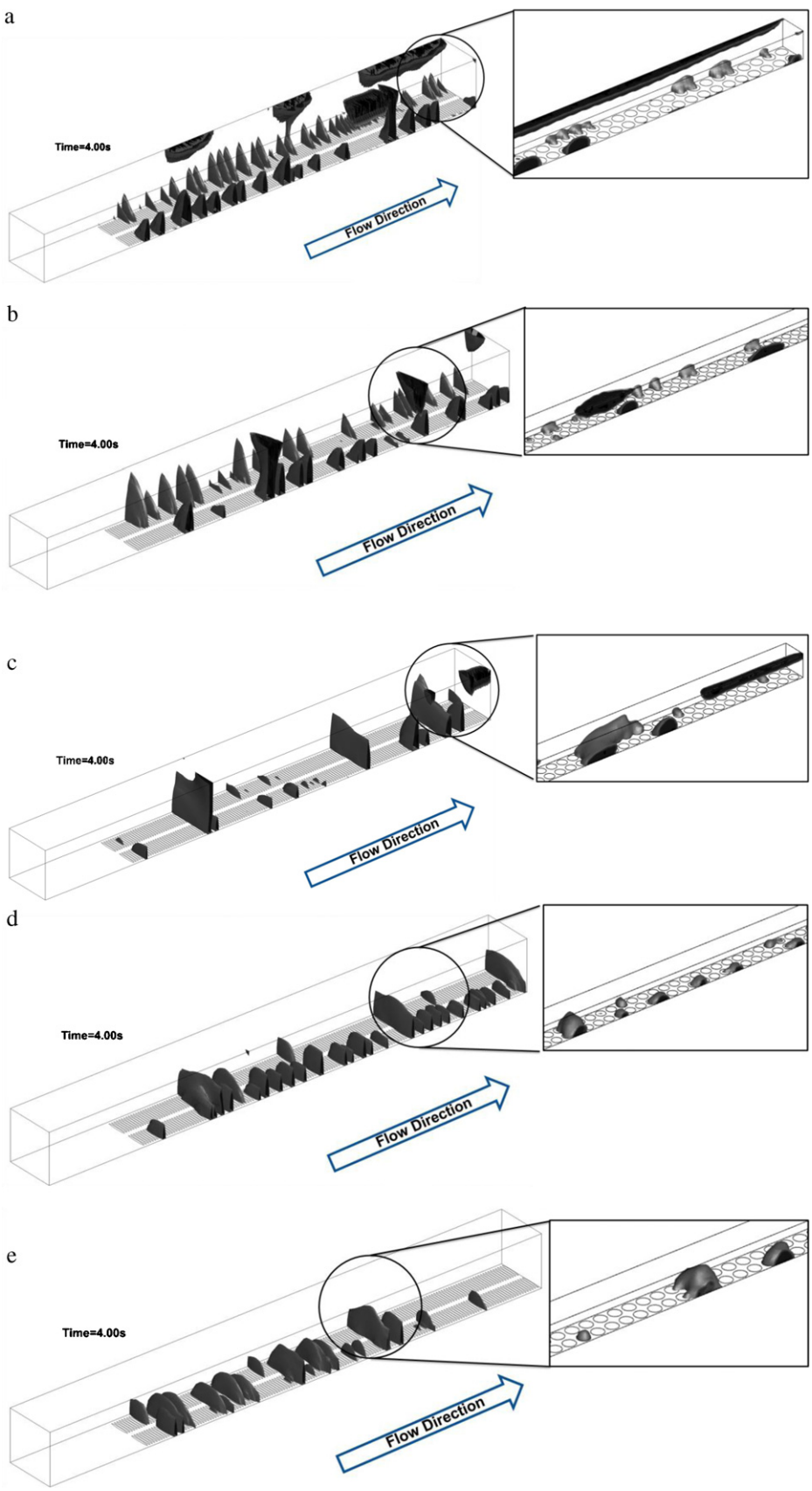

Fig. 10. Effects of contact angle of channel side and top wall surfaces on the two-phase flow patterns in the channel: (a) $\theta = 45^\circ$, (b) $\theta = 60^\circ$, (c) $\theta = 90^\circ$, (d) $\theta = 120^\circ$, (e) $\theta = 140^\circ$.

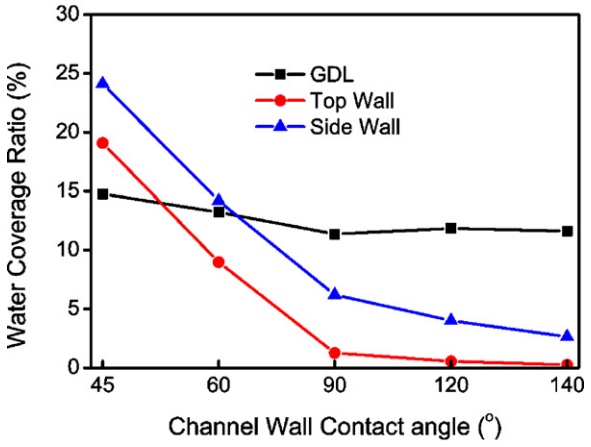

Fig. 11. Effects of channel wall contact angle on the water distribution in the channel.

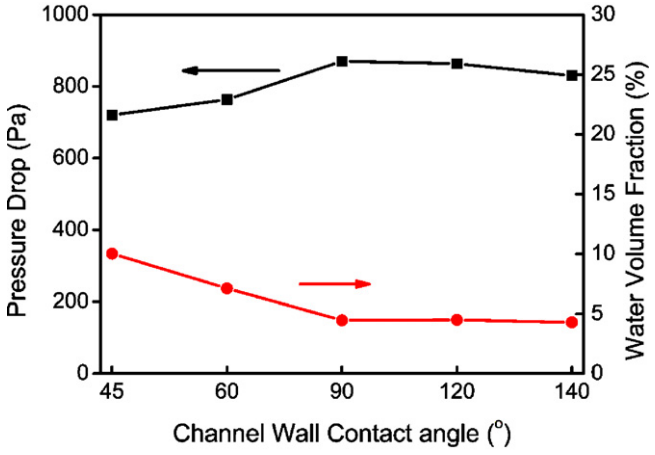

Fig. 12. Effects of channel wall contact angle on the pressure drop and water volume fraction in the channel.

the water volume fraction in the channel, because of the reduced water resident time. The previous results indicate that using a more hydrophilic channel wall is helpful to reduce the pressure drop but the GDL water coverage ratio also increases slightly. The selection of optimal channel wall wettability thus depends on the specific requirement of fuel cell applications.

4. Conclusions

4.1. The following conclusions can be drawn from this study

1) Three stages of droplet behavior can be identified, namely, (i) emergence and merging of liquid water on the GDL surface, (ii) accumulation on the side walls, and iii) detachment from the top wall,. For the base case, i.e., at theoretical liquid water production rate, the flow pattern is corner droplet flow, with liquid water mainly presents in the bottom corners.
2) With increasing liquid injection rates, the flow pattern evolves from corner droplet flow to top wall film flow, annular flow, and finally slug flow.
3) To reduce the parasitic energy loss, the water volume faction should be kept as low as possible in the channel, since the pressure drop increases exponentially with it.
4) The material wettability has a great impact on the two-phase flow pattern, water distribution and pressure drop. Using a more hydrophobic GDL surface is helpful to expel water from the GDL surface, but may also increase the pressure drop. On the other hand, using a more hydrophilic channel wall reduces the pressure drop, but increases the GDL water coverage ratio slightly and the water residence time.

Acknowledgment

The authors are grateful to the Natural Science and Engineering Research Council of Canada (NSERC) for a Strategic Grant to support this study.

References

[1] R. Anderson, L. Zhang, Y. Ding, M. Blanco, X. Bi, D.P. Wilkinson, J. Power Sources 195 (2010) 4531–4553.
[2] X. Liu, H. Guo, F. Ye, C.F. Ma, Int. J. Hydrogen Energy 33 (2008) 1040–1051.
[3] I.S. Hussaini, C.Y. Wang, J. Power Sources 187 (2009) 444–451.
[4] Z.W. Dunbar, R.I. Masel, J. Power Sources 182 (2008) 76–82.
[5] Z. Lu, S.G. Kandlikar, C. Rath, M. Grimm, W. Domigan, A.D. White, M. Hardbarger, J.P. Owejan, T.A. Trabold, Int. J. Hydrogen Energy 34 (2009) 3445–3456.
[6] L. Zhang, H.T. Bi, D.P. Wilkinson, J. Stumper, H. Wang, J. Power Sources 195 (2010) 3231–3239.
[7] L. Zhang, H.T. Bi, D.P. Wilkinson, J. Stumper, H. Wang, J. Power Sources 183 (2008) 643–650.
[8] L. Zhang, W. Du, H.T. Bi, D.P. Wilkinson, J. Stumper, H. Wang, J. Power Sources 189 (2009) 1023–1031.
[9] R. Anderson, D.P. Wilkinson, X. Bi, L. Zhang, J. Power Sources 195 (2010) 4168–4176.
[10] J. Chen, J. Power Sources 195 (2010) 1122–1129.
[11] A. Bazylak, Int. J. Hydrogen Energy 34 (2009) 3845–3857.
[12] A.Z. Weber, J. Newman, Chem. Rev. 104 (2004) 4679–4726 (Washington, DC, U. S.).
[13] C.Y. Wang, Chem. Rev. 104 (2004) 4727–4765 (Washington, DC, U. S.).
[14] Z.H. Wang, C.Y. Wang, K.S. Chen, J. Power Sources 94 (2001) 40–50.
[15] S. Mazumder, J.V. Cole, J. Electrochem. Soc. 150 (2003) A1503–A1509, A1503-A1509.
[16] T. Berning, N. Djilali, J. Electrochem. Soc. 150 (2003) A1589–A1598, A1589-A1598-.
[17] V. Gurau, Mann Jr., J. Electrochem. Soc. 157 (2010) B512–B521, B512- B521-.
[18] P. Quan, B. Zhou, A. Sobiesiak, Z.S. Liu, J. Power Sources 152 (2005) 131–145.
[19] A. Theodorakakos, T. Ous, A. Gavaises, J.M. Nouri, N. Nikolopoulos, H. Yanagihara, J. Colloid Interface Sci. 300 (2006) 673–687.
[20] Z. Zhan, J. Xiao, M. Pan, R. Yuan, J. Power Sources 160 (2006) 1–9.
[21] E. Shirani, S. Masoomi, J. Fuel Cell Sci. Technol. 5 (2008) 041008–141008.
[22] Y.H. Cai, J. Hu, H.P. Ma, B.L. Yi, H.M. Zhang, J. Power Sources 161 (2006) 843–848.
[23] X. Zhu, P.C. Sui, N. Djilali, J. Power Sources 172 (2007) 287–295.
[24] A. Bazylak, D. Sinton, N. Djilali, J. Power Sources 176 (2008) 240–246.
[25] X. Zhu, P.C. Sui, N. Djilali, Microfluid. Nanofluid. 4 (2008) 543–555.
[26] X. Zhu, P.C. Sui, N. Djilali, J. Power Sources 181 (2008) 101–115.
[27] C. Fang, C. Hidrovo, F.-m. Wang, J. Eaton, K. Goodson, Int. J. Multiphase Flow 34 (2008) 690–705.
[28] P. Quan, B. Zhou, A. Sobiesiak, Z. Liu, J. Power Sources 152 (2005) 131–145.
[29] K. Jiao, B. Zhou, P. Quan, J. Power Sources 154 (2006) 124–137.
[30] K. Jiao, B. Zhou, P. Quan, J. Power Sources 157 (2006) 226–243.
[31] P. Quan, M.C. Lai, J. Power Sources 164 (2007) 222–237.
[32] A.D. Le, B. Zhou, J. Power Sources 182 (2008) 197–222.
[33] A.D. Le, B. Zhou, Electrochim. Acta 54 (2009) 2137–2154.
[34] Y. Ding, H.T. Bi, D.P. Wilkinson, J. Power Sources 195 (2010) 7278–7288.
[35] B. Sundeĩn, Transport phenomena in fuel cells, WIT Press, Boston, 2005.
[36] FLUENT 6.3 UDF Manual, 2006.
[37] A.D. Le, B. Zhou, H.R. Shiu, C.I. Lee, W.C. Chang, J. Power Sources 195 (2010) 7302–7315.
[38] D. Bevers, R. Rogers, M. von Bradke, J. Power Sources 63 (1996) 193–201.
[39] C. Lim, C.Y. Wang, Electrochim. Acta 49 (2004) 4149–4156.